

Supplementary Information

Observation of magnon polarons in van-der-Waals itinerant ferromagnet Fe_3GeTe_2

Qili Li^{1,*†}, Namrata Bansal^{1,*}, Paul Nufer¹, Lichuan Zhang^{2,3}, Amir-Abbas Haghighirad⁴,
Christoph Sürgers¹, Yuriy Mokrousov^{3,5}, and Wulf Wulfhekel^{1,4}

¹Physikalisches Institut, Karlsruhe Institute of Technology, Karlsruhe, Germany

²School of Physics and Electronic Engineering, Jiangsu University, Zhenjiang, China

³Peter Grünberg Institut (PGI-1) and Institute for Advanced Simulation (IAS-1)
Forschungszentrum Jülich GmbH, Jülich, Germany

⁴Institute for Quantum Materials and Technologies, Karlsruhe Institute of Technology,
Karlsruhe, Germany

⁵Institute of Physics, Johannes Gutenberg-University Mainz, Mainz, Germany

*These authors contributed equally to this work.

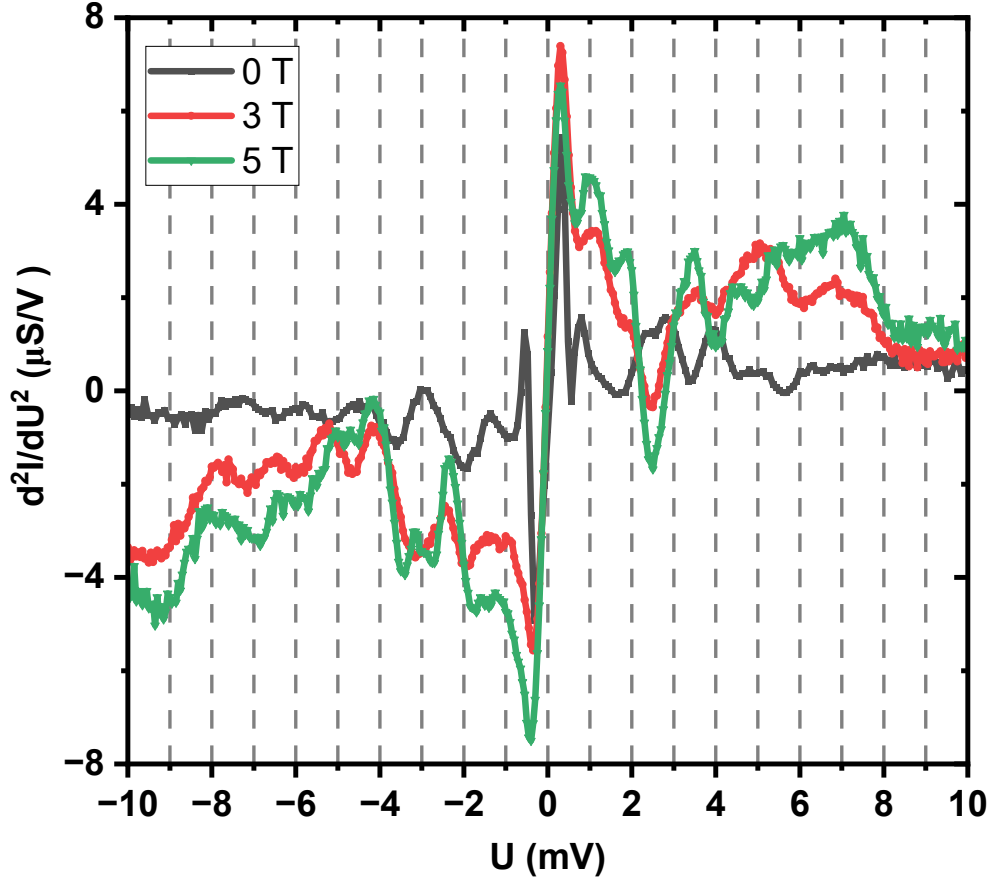
†Corresponding author: qili.li@kit.edu

Contents

1	Magnetic-field dependence of quasiparticle excitations	2
2	Temperature dependence of quasiparticle excitations	3
3	Identify magnon-phonon band crossings	3
4	Model calculations for optical phonon with and without magnon-phonon coupling	4
5	Temperature dependence of the in-plane electrical resistivity of the Fe_3GeTe_2 single crystal	4

1 Magnetic-field dependence of quasiparticle excitations

Here we present the magnetic-field dependence of magnon polaron excitations under an out-of-plane magnetic field up to 5 T measured with W tip at 45 mK. The magnetic field shifts the magnon dispersion up because of the Zeeman energy, whereas the phonon dispersion is independent of the magnetic field. Note that the 0.3 mV does not change with magnetic field, which originates from the dynamical Coulomb blockade [1–4].



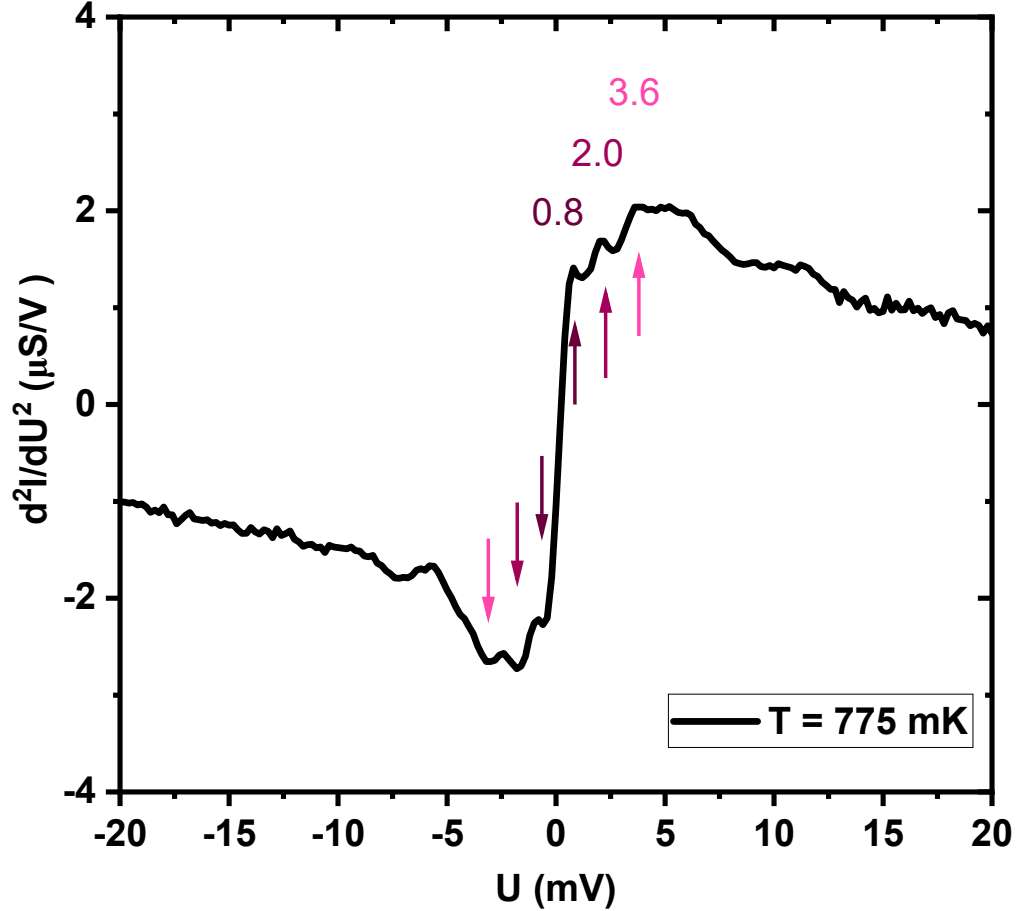
Supplementary Figure 1: Magnetic-field dependence. d^2I/dU^2 measured at 45 mK under different magnetic fields at 0 T (black curve), 3 T (red curve), and 5 T (green curve). The tunneling conditions: 0 T ($U = 20$ mV, $I = 2$ nA with $U_{\text{mod}}=0.5$ mV), 3 T ($U = 10$ mV, $I = 2$ nA with $U_{\text{mod}}=0.5$ mV), 5 T ($U = 10$ mV, $I = 2$ nA with $U_{\text{mod}}=0.5$ mV). The modulation frequency was 3.421 kHz the same for different magnetic field.

With magnon-phonon coupling, magnon polarons emerge at the avoided band crossings, leading to an enhanced inelastic signal at the energy of the band crossing. The band crossings shift in energy in a magnetic field in a complex way. In case the magnon dispersion is flatter than the phonon dispersion, i.e. at low energies, the application of an out-of plane magnetic fields increases the magnon energy and the crossing point with the phonon branch shifts to higher energies and higher momenta (see e.g. Fig. 4d, low energy crossing at 0.8 meV). In the opposite case of a steeper magnon dispersion, the up-shift of the magnon dispersion shifts the crossing point to lower momentum and the energy of the crossing shifts downward (see e.g. Fig. 4b, crossing at 5.2 meV).

At energies, where both dispersions are tangential, the crossings may disappear with the field (see e.g. Fig. 4b and c between 1.2 and 2.5 meV). Indeed, we observed this behavior of the inelastic peaks in the dI^2/dU^2 spectra under different magnetic fields.

2 Temperature dependence of quasiparticle excitations

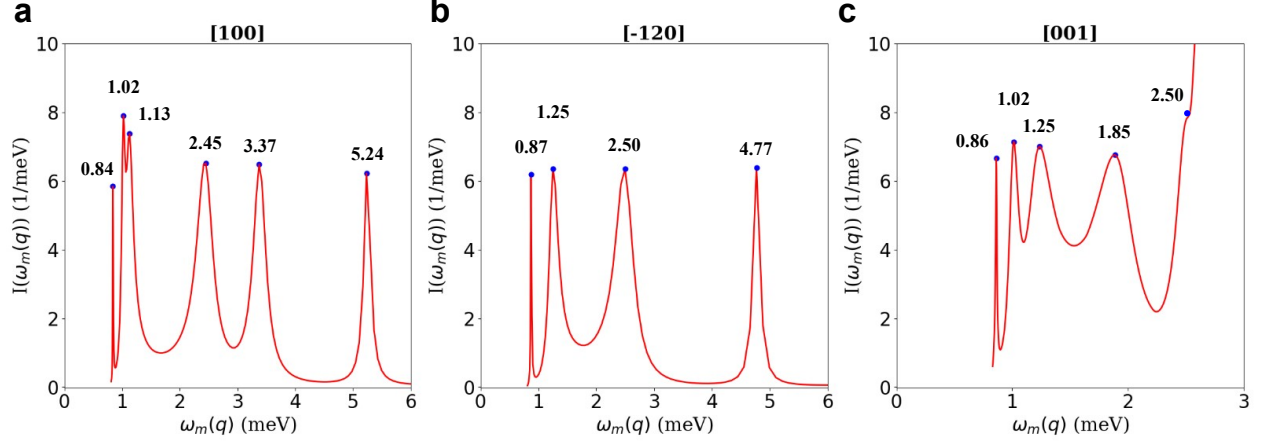
Supplementary Figure 2 shows low-energy excitations at 775 mK with W tip. The thermal broadening smears the peaks at 0.8, 2.3, 3.8 and 5.1 meV (Fig. 1d), where a broad peak can be seen as shown in Supplementary Fig. 2. We can expect that at even higher temperature all the individual peaks will merge as one broad peak.



Supplementary Figure 2: Temperature dependence. dI^2/dU^2 spectra measured at 775 mK . The tunneling condition was $U = 20$ mV, $I = 3$ nA, and $U_{\text{mod}}=1$ mV at 6.551 kHz.

3 Identify magnon-phonon band crossings

With the dispersions of the phonon and the magnon, we calculated their band crossings as follows. We defined an intensity function to characterize the band crossings. $I(\omega_m(q)) = \sum_{\nu} \frac{\eta}{(\omega_m(q) - \omega_p^{\nu}(q))^2 + \eta^2}$, with a small broadening parameter $\eta = 0.05$ meV. ν is the phonon band index. A peak appears in $I(\omega_m(q))$ when the phonon band crosses with the magnon band ($\omega_p(q) = \omega_m(q)$).



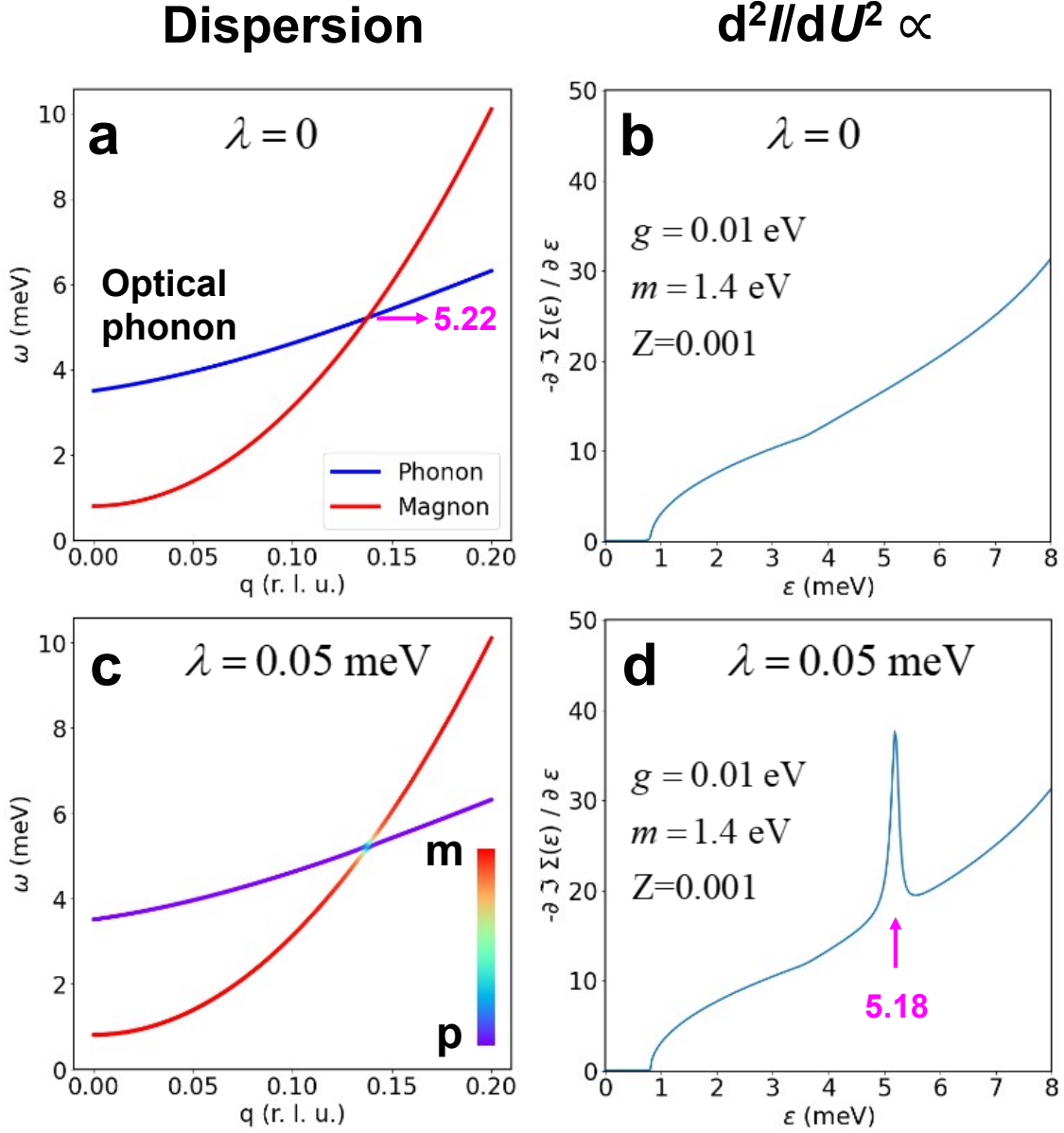
Supplementary Figure 3: Identify magnon-phonon band crossings. **a-c** are band crossings in $[100]$, $[-120]$ and $[001]$ directions, respectively.

4 Model calculations for optical phonon with and without magnon-phonon coupling

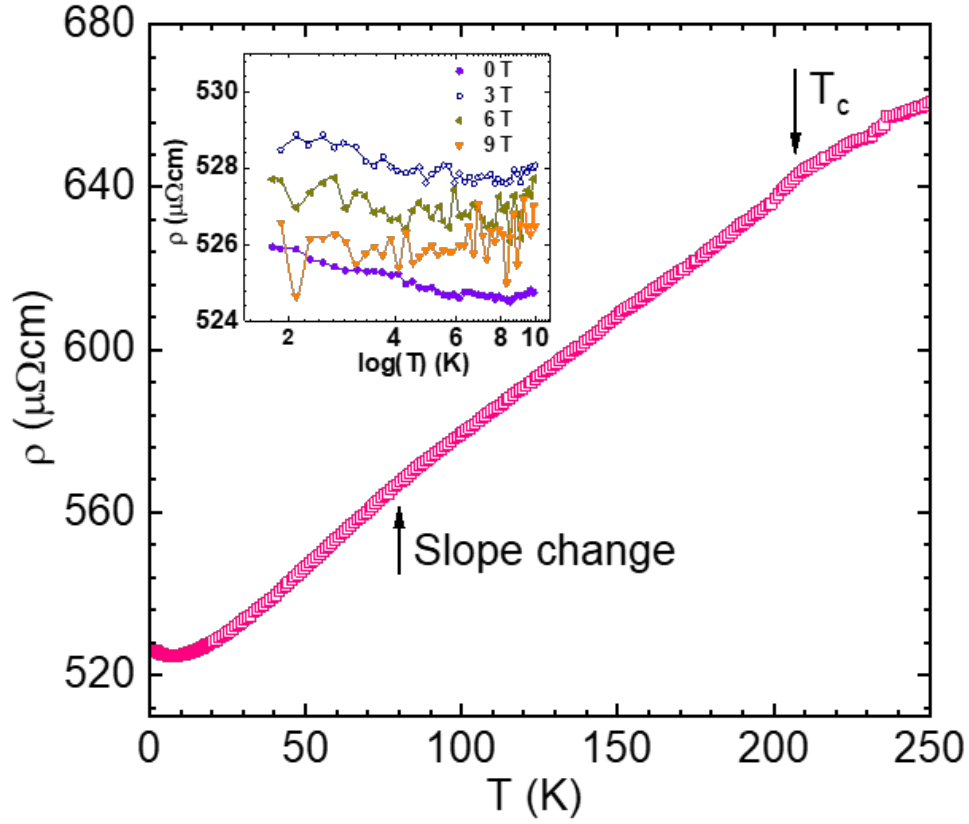
Here we demonstrate that the lowest optical phonon band crosses with the magnon band, resulting in the magnon polaron excitation at 5.18 meV which agrees with our experimental results very well. The parameters used for the model calculations are the same with Figure 5 in the maintext. Generally, the optical phonon has one crossing with magnon band. In the case of magnon-phonon coupling, the avoided crossing results a peak in ISTS.

5 Temperature dependence of the in-plane electrical resistivity of the Fe_3GeTe_2 single crystal

We measured the temperature dependence of the in-plane electrical resistivity of the Fe_3GeTe_2 single crystal (Supplementary Fig. 5). We discussed about the influence of magnon-phonon coupling on electric resistivity here. Electric resistivity in metals is caused by the inelastic scattering of hot carriers off bosonic excitations of the crystal, i.e. off phonons and in magnetic materials additionally off magnons. In a conventional description of these scattering processes, the dispersion and bosonic density of states of the two are treated separately. While this is usually a good approximation, the situation changes in 2D systems with sufficient magnetoelastic coupling, i.e. typically when large magnetocrystalline anisotropies couple the spin and lattice degree of freedom. In this case, phonons and magnons hybridize near band crossings. The hybridized magnon polarons can, however, much more efficiently couple to the conduction electrons, as the strict spin selection rules are lifted. As a consequence, a larger temperature dependence is expected than from phonons, alone, in the relevant temperature ranges. Supplementary Figure 5 displays the resistivity measured after magnetically saturating the FGT sample followed by warming up, displaying a sizable increase of resistivity above about 10 K and a kink at the Curie temperature. Notably, there is no clear maximum of the resistivity observed that would indicate a Kondo lattice behavior [5, 6]. A weak change of slope can, however, be seen around 80 K, which roughly corresponds to a thermal energy of the highest observed phonon-magnon crossing point and the resistivity is almost constant below about 9 K, corresponding to thermal energies below the lowest hybridization point.



Supplementary Figure 4: Model calculations for optical phonon without and with magnon-phonon coupling. **a** Band crossing for magnon and optical phonon. **b** The derivative of electron self-energy without magnon-phonon coupling. **c** Avoided band crossing between magnon and optical phonon. **d** The derivative of electron self-energy i.e., ISTS for magnon polaron.



Supplementary Figure 5: Temperature dependence of the in-plane electrical resistivity of the Fe_3GeTe_2 single crystal. Resistivity vs temperature after magnetically saturating the FGT sample followed by warming up. Inset shows the semi-logarithmic plot of the resistivity at low temperatures under different magnetic fields.

References

- [1] Michael Schackert, Tobias Märkl, Jasmin Jandke, Martin Hölzer, Sergey Ostanin, Eberhard KU Gross, Arthur Ernst, and Wulf Wulfhekel. Local measurement of the eliashberg function of pb islands: Enhancement of electron-phonon coupling by quantum well states. *Phys. Rev. Lett.*, 114(4):047002, 2015.
- [2] Christian R. Ast, Berthold Jäck, Jacob Senkpiel, Matthias Eltschka, Markus Etzkorn, Joachim Ankerhold, and Klaus Kern. Sensing the quantum limit in scanning tunnelling spectroscopy. *Nat. Commun.*, 7(1):13009, 2016.
- [3] J. Senkpiel, J. C. Klockner, M. Etzkorn, S. Dambach, B. Kubala, W. Belzig, A. L. Yeyati, J. C. Cuevas, F. Pauly, J. Ankerhold, C. R. Ast, and K. Kern. Dynamical coulomb blockade as a local probe for quantum transport. *Phys. Rev. Lett.*, 124(15):156803, 2020.
- [4] Taner Esat, Markus Ternes, Ruslan Temirov, and F. Stefan Tautz. Electron spin secluded inside a bottom-up assembled standing metal-molecule nanostructure. *Phys. Rev. Res.*, 5:033200, Sep 2023.
- [5] M. Lavagna, C. Lacroix, and M. Cyrot. Electrical resistivity of the kondo lattice. *Journal of Applied Physics*, 53(3):2055–2057, 1982.
- [6] Yun Zhang, Haiyan Lu, Xiegang Zhu, Shiyong Tan, Wei Feng, Qin Liu, Wen Zhang, Qiuyun Chen, Yi Liu, Xuebing Luo, et al. Emergence of kondo lattice behavior in a van der waals itinerant ferromagnet, fe3gete2. *Sci. Adv.*, 4(1):eaao6791, 2018.